# OBSERVATIONS OF WIND/WAVE DRAG ON THE BIO BARREL DRIFTER AND OTHER SURFACE DRIFTERS

J.A. Elliott

Science Branch, Maritimes Region
Ocean and Ecosystem Sciences Division
Fisheries and Oceans Canada
1 Challenger Drive
Dartmouth, NS
B2Y 4A2

2018

**Canadian Technical Report of Fisheries and Aquatic Sciences 3257**

Fisheries and Oceans Canada | Pêches et Océans Canada

Canada

**Canadian Technical Report of Fisheries and Aquatic Sciences**

Technical reports contain scientific and technical information that contributes to existing knowledge but which is not normally appropriate for primary literature. Technical reports are directed primarily toward a worldwide audience and have an international distribution. No restriction is placed on subject matter and the series reflects the broad interests and policies of Fisheries and Oceans Canada, namely, fisheries and aquatic sciences.

Technical reports may be cited as full publications. The correct citation appears above the abstract of each report. Each report is abstracted in the data base *Aquatic Sciences and Fisheries Abstracts*.

Technical reports are produced regionally but are numbered nationally. Requests for individual reports will be filled by the issuing establishment listed on the front cover and title page.

Numbers 1-456 in this series were issued as Technical Reports of the Fisheries Research Board of Canada. Numbers 457-714 were issued as Department of the Environment, Fisheries and Marine Service, Research and Development Directorate Technical Reports. Numbers 715-924 were issued as Department of Fisheries and Environment, Fisheries and Marine Service Technical Reports. The current series name was changed with report number 925.

**Rapport technique canadien des sciences halieutiques et aquatiques**

Les rapports techniques contiennent des renseignements scientifiques et techniques qui constituent une contribution aux connaissances actuelles, mais qui ne sont pas normalement appropriés pour la publication dans un journal scientifique. Les rapports techniques sont destinés essentiellement à un public international et ils sont distribués à cet échelon. Il n'y a aucune restriction quant au sujet; de fait, la série reflète la vaste gamme des intérêts et des politiques de Pêches et Océans Canada, c'est-à-dire les sciences halieutiques et aquatiques.

Les rapports techniques peuvent être cités comme des publications à part entière. Le titre exact figure au-dessus du résumé de chaque rapport. Les rapports techniques sont résumés dans la base de données *Résumés des sciences aquatiques et halieutiques*.

Les rapports techniques sont produits à l'échelon régional, mais numérotés à l'échelon national. Les demandes de rapports seront satisfaites par l'établissement auteur dont le nom figure sur la couverture et la page du titre.

Les numéros 1 à 456 de cette série ont été publiés à titre de Rapports techniques de l'Office des recherches sur les pêcheries du Canada. Les numéros 457 à 714 sont parus à titre de Rapports techniques de la Direction générale de la recherche et du développement, Service des pêches et de la mer, ministère de l'Environnement. Les numéros 715 à 924 ont été publiés à titre de Rapports techniques du Service des pêches et de la mer, ministère des Pêches et de l'Environnement. Le nom actuel de la série a été établi lors de la parution du numéro 925.

Fisheries and Oceans Canada | Pêches et Océans Canada

Canada

Canadian Technical Report of
Fisheries and Aquatic Sciences 3257

2018

# Observations of Wind/Wave Drag on the BIO Barrel Drifter and Other Surface Drifters

by

J.A. Elliott[1]

Department of Fisheries and Oceans
Bedford Institute of Oceanography
Dartmouth, Nova Scotia

[1] Retired

© Her Majesty the Queen in Right of Canada, 2018.

Cat. No. Fs 97-6/3257E-PDF ISBN 978-0-660-25518-7 ISSN 1488-5379

Correct citation for this publication:

Elliott, J.A. 2018. Observations of Wind/Wave Drag on the BIO Barrel Drifter and Other Surface Drifters. Can. Tech. Rep. Fish. Aquat. Sci. 3257: v + 40p.

TABLE OF CONTENTS

TABLE OF CONTENTS ..... iii
ABSTRACT ..... iv
RÉSUMÉ ..... iv
ACKNOWLEDGEMENTS ..... v
1. INTRODUCTION ..... 1
2. BIO BARREL DRIFTER ..... 3
3. WIND/WAVE DRAG ..... 4
4. FIELD TRIALS and ERROR ANALYSIS ..... 6
5. DRIFT SPEED for X, S, M, and L ..... 9
6. DRIFT SPEED for S, ½ S, ½ M, and ½ L ..... 13
7. DRIFT SPEED of S and $S_{10}$ ..... 15
8. DRIFT SPEED of $S_{10}$ with ½ $S_{10}$ and ¼ $S_{10}$ ..... 16
9. DRIFT SPEED of OTHER BUOYS ..... 16
10. COMPOSITE of BEDFORD BASIN TRIALS ..... 17
11. DRIFT SPEED in OCEAN TRIALS ..... 19
12. CONCLUSIONS ..... 20
13. REFERENCES ..... 23
14. APPENDIX 1: Scatter Plots of $\Delta v$ for Pairs of Buoys ..... 24

## ABSTRACT

Elliott, J.A. 2018. Observations of Wind/Wave Drag on the BIO Barrel Drifter and Other Surface Drifters. Can. Tech. Rep. Fish. Aquat. Sci. 3257: v + 40p.

To aid development of numerical models and have real time environmental monitoring of surface currents, BIO designed a Lagrangian surface drifter, the BIO Barrel Drifter, for use in the near shore and open ocean. This is a documentation of the results from field trials undertaken to find the wind/wave drag influence on the drift speed. Based on these trials, the drift speed of the BIO Barrel Drifter can be corrected for wind/wave drag error to better than ±1 cm/sec. Other surface drifters, some commercial, are included in the analysis.



## RÉSUMÉ

Elliott, J.A. 2018. Observations relatives à la résistance au vent/aux vagues des bouées dérivantes de l'Institut océanographique de Bedford et d'autres bouées dérivantes. Can. Tech. Rep. Fish. Aquat. Sci. 3257: v + 40p.

Afin d'aider dans l'élaboration de modèles numériques et d'assurer une surveillance en temps réel des courants de surface, l'Institut océanographique de Bedford (IOB) a conçu une bouée lagrangienne, la bouée dérivante de l'IOB, aux fins d'utilisation près du rivage et en haute mer. Le présent document fait était des résultats des essais réalisés sur le terrain afin de déterminer l'effet de la résistance au vent/aux vagues sur la vitesse de dérive. À la suite de ces essais, les erreurs de vitesse de dérive de la bouée dérivante de l'IOB découlant de la résistance au vent/aux vagues peuvent être corrigées à ±1 cm/s. L'analyse comprend également d'autres bouées dérivantes, dont certains sont des modèles commerciaux.

ACKNOWLEDGEMENTS

The unpublished report, White, et al. (1983), which is the source of data for this analysis, had incremental funding provided by the NRCan 'Panel of Energy Research and Development' (PERD) and by the Canadian Offshore Oil Spill Research Association (COOSRA), an industry consortium. G.A. Fowler designed the 'BIO Barrel Drifter', contributed to its successful evaluation, and provided graphics. W.D. White, under contract from a local firm, was responsible for overall coordination of the field activities. Numerous professional and technical staff from throughout BIO and from the Canadian Coast Guard, Dartmouth, aided or participated in the field work. Thanks to Ross Hendry and Herb Vandermeulen for their reviews.

# 1. INTRODUCTION

Throughout history the curious have enjoyed using 'drifters' to monitor the motion of water. At BIO that history continues with the use of the 'BIO Barrel Drifter' to monitor ocean surface currents. Present deployment is in the vicinity of Port Hawkesbury, Nova Scotia, as part of a program to improve oil spill prevention and response plans of several major shipping ports (Drozdowski, et al. 2017), a component of the World Class Tanker Safety Systems (WCTSS) program. The basic tool being used for current measurements is a moored Acoustic Doppler Current Profiler (ADCP). However, ADCPs have uncertain accuracy in the upper 10% of the water column. The 'BIO Barrel Drifter', a Lagrangian surface drifter, is a supplement to improve knowledge of this upper layer. A Lagrangian drifter will follow a path defined by the net of wind and water forces experienced. This analysis focuses on a field study on how the BIO Barrel Drifter responds to wind/wave drag on the antenna. For compatibility with the ADCPs, an accuracy of about ±1 cm/sec for 'surface current' is desired.

Details on the field program are published in a companion data document, Elliott and Fowler (2018); a revitalized version of an earlier 1980's unpublished data report White et al. (1983). During 1980 to 1985, a series of field trials were held in the Bedford Basin to measure the influence of wind/wave drag on the above-surface component (mast/antenna) of various drifter designs. In addition to the BIO Barrel Drifter, five other surface drifters (some commercial) were included: Hermes Drifter, Orion 4800, Nova Tech 200RF, Orion Tracker and BIO Tarball Tracker. Schematic diagrams of all the types evaluated are shown in Figure 1.

The BIO Barrel design is intended to be suitable for deployment in the near offshore, employing available satellite tracking, to track surface drift in the upper metre. Operational and scientific needs were influenced by the experience with oil dispersion from the grounding of the tanker Arrow, see Forrester (1971). The different versions of BIO drifter shown in Figure 1 were used to explore drift behaviour with controlled changes in mast diameter and barrel depth.

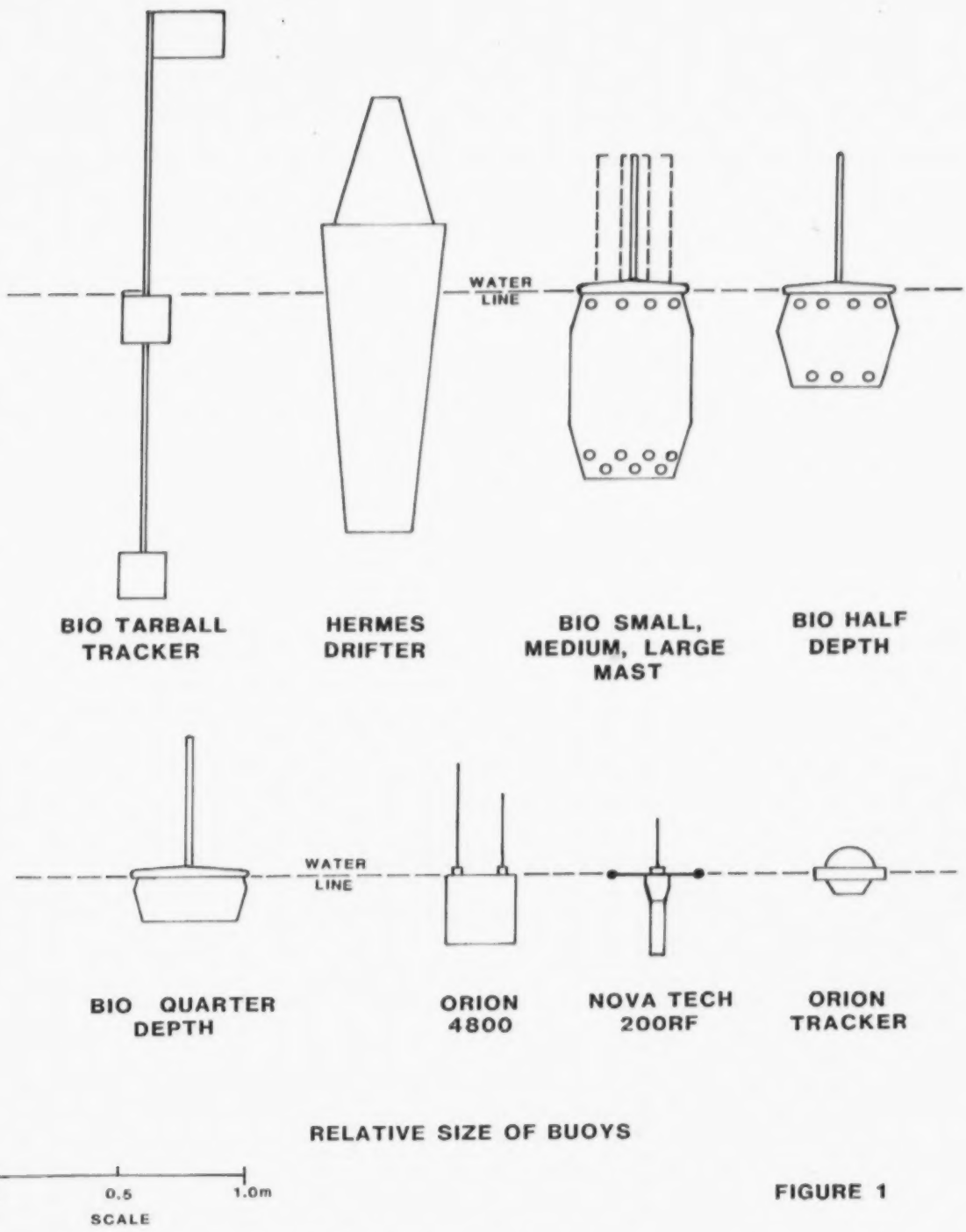


Figure 1: Schematic diagrams of the drifters included in the trials.

## 2. BIO BARREL DRIFTER

The BIO Barrel design is a barrel shaped sub-surface buoy adjusted for near neutral buoyancy. Mounted on top is an above-surface cylindrical mast (antenna). Figure 2 is a cut-away 3-D diagram. Four versions of the BIO Barrel Drifter were constructed. Buoy L is for large diameter antenna, M for medium diameter, S for small diameter, and X for no antenna. Version M is the intended final design. Through comparison of relative drift rates between pairs, the influence of wind drag is deduced. The depth of the barrel was chosen to be appropriate for a drifter tracking

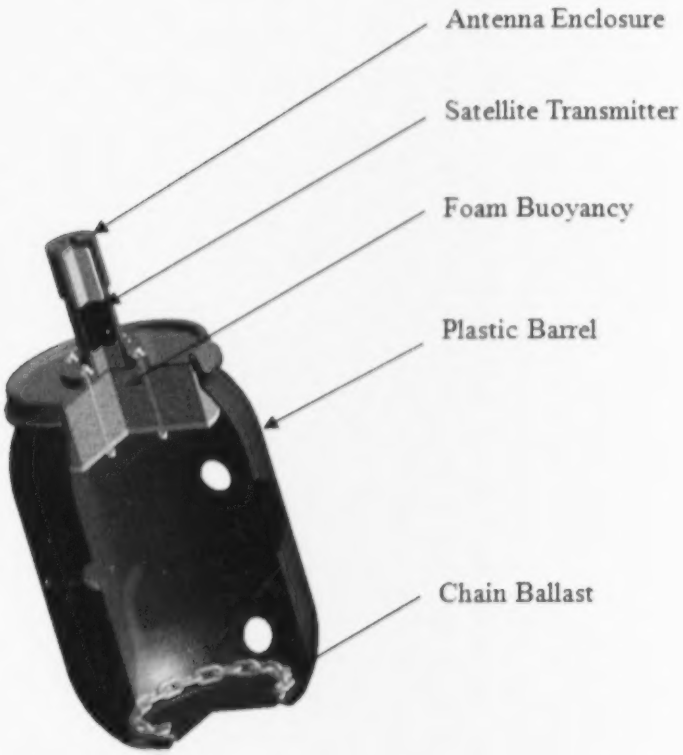


Figure 2: Cutaway diagram of the BIO Barrel Drifter. Buoyancy and ballast are adjusted for in-air weight of 20 kg and freeboard of 2 cm. During field trials, the antenna enclosure had three different diameters, and the barrel three different depths. See Table 1 for details of dimensions. Figure from Elliott and Fowler (2018).

the motion in the top half metre of the water column. The antennas are identical except for diameter. Antenna size of buoy M was that required to accommodate satellite tracking hardware at that time; see Table 1. The barrel free-board was adjusted to be about 2 cm. With the relatively large surface area of the top of the barrel, the buoy is a good surface follower. The low surface profile (small free-board) of the barrel is desirable to keep any unwanted wind/wave drag at a minimum. Ballasting to minimize tilt and resonance effects was a concern. After initial field trials the weight was adjusted. As a result, there are two sections in the field trials: an initial group of data where the in-air weight is recorded as 10 kg and a follow-on set with a heavier ballast of 20 kg or 30 kg. The following analysis uses data from both versions with the preferred heavier ballast version taken as the more accurate.

**Table 1**

| Buoy antenna type | Large L | Medium M | Small S | None X |
|---|---|---|---|---|
| | | | | |
| Antenna diameter | 29 cm | 10 cm | 2.4 cm | 0 |
| Antenna height | 59.5 cm | 59.5 cm | 59.5 cm | 0 |
| $A_a$ Antenna x-sectional area | 1725.5 $cm^2$ | 595 $cm^2$ | 142.8 $cm^2$ | 0 |
| | | | | |
| Barrel diameter | 44 cm | 44 cm | 44 cm | 44 cm |
| Barrel height | 77.5 cm | 77.5 cm | 77.5 cm | 77.5 cm |
| $A_o$ Barrel x-sectional area | 3410 $cm^2$ | 3410 $cm^2$ | 3410 $cm^2$ | 3410 $cm^2$ |
| | | | | |
| $A_a/A_o$ | 0.501 | 0.174 | 0.042 | 0 |
| | | | | |
| $\{ A_a/A_o \}^{1/2}$ | 0.71 | 0.42 | 0.20 | 0 |
| | | | | |

## 3. WIND/WAVE DRAG

For buoy X, no antenna, the barrel float will drift balancing the drag over its depth. Averaging vertical shear currents over its 77.5 cm depth would represent a mean current at about 40 cm depth. The addition of a mast or antenna results in a wind/wave force which produces an increase in mean speed, v; this adds drag sufficient to balance the wind force. With an axis fixed

to the buoy, y vertical, this balance of forces can be described using the standard equation for total form drag, $F = \frac{1}{2} \rho_o C_o A V^2$, (Daugherty and Ingersoll 1954) as:

$$\frac{1}{2} \rho_a C_a A_a U^2(y) = \frac{1}{2} \rho_o C_o A_o v^2$$

where $\rho_a$, $\rho_o$, $C_a$, and $C_o$ are density and drag coefficient for a-air and o-ocean, A is the cross-sectional area of the antenna or the buoy, U(y) wind speed along the antenna and v the resulting incremental increase in speed of the barrel. The densities of the air and the ocean can be taken as constants. For both the antenna and the barrel the drag coefficients, based on two dimensional cylinders (Daugherty and Ingersoll 1954), are essentially constant for the Reynolds Number(s) expected, approximately $10^2$ to $3 \times 10^5$. Over this range it varies by about $\pm$ 10 %. For a wind at 1/2 m height of 5 m/s, and v as 3 cm/s, the Reynolds Number for the antenna is $2 \times 10^5$ maximum, and for the barrel, $6 \times 10^3$. Advantage can be taken of the near constant drag coefficients to simplify the force balance formula.

The above can be rearranged to:

$$K\, U(y) \{A_a / A_o\}^{1/2} = v$$

where, for the average of Reynolds Numbers expected based on the wind speeds during the trials, K is a near constant with maximum variability of about $\pm$10 % or less. This variability will be a second order effect relative to the planned changes in $A_a$.

For the four types of drifters L, M, S, and X, the cross-sectional area of the barrel, $A_o$, is a constant (Table 1). Thus for a given wind profile U(y), there is a simple near proportional linear relationship between $\{A_a\}^{1/2}$ and v.

The field trials were conducted with combinations of antenna sizes to experimentally determine the relation between $\{A_a / A_o\}^{1/2}$ and v. Pairs of buoy types to be compared were deployed sufficiently close together that mean currents, such as wind drift and tidal flow, were expected to be identical. Two buoy clusters, drifting at velocity $V_i$, with different 'antenna', will have a separation velocity $\Delta v_{\{1\text{-}2\}}$ as

$$\Delta v_{\{1\text{-}2\}} = (V_1 - V_2), \text{ and } V_i = \Delta d_i / \Delta t_i$$

where $\Delta d_i$ and $\Delta t_i$ are the distance and time difference between position fixes. The core data for analysis are the positions and times for each pair of buoy types deployed. Table 2 lists the final

results from the pair comparisons. In the first column 'Buoy Type' the letters, as described above, are codes identifying the different experimental versions of the BIO Barrel Drifter. The fractions are the reduced barrel depth, and the subscripts are for a different ballast. The names refer to the non-BIO Barrel drifters. The second column is the number of independent trials for that pair. The heading on the following four columns are the BIO buoy used as reference. Values in the table are the Δv in m/min. Detail on the analysis for each follows below. The final column is the ratio of cross sectional area as defined above.

**Table 2**

Average Δv metres/minute at $U_{10}$ 10 metres/sec

| Buoy Type | # Trials | X ref | S ref | $S_{10}$ ref | 1/2S ref | $[A_a/A_o]^{1/2}$ |
|---|---|---|---|---|---|---|
| X | 5 | | | 3.47* | | 0 |
| S | 25 | 1.94 | | | | 0.206 |
| M | 7 | 4.34 | 2.4 | | | 0.438 |
| L | 7 | 6.84 | 4.9 | | | 0.714 |
| 1/2S | 5 | | 2.69 | | | 0.292 |
| 1/2M | 5 | | 5.64 | | 2.95 | 0.620 |
| 1/2L | 5 | | 8.97 | | 6.28 | 1.01 |
| $S_{10}$ | 12 | 3.47 | 1.53 | | | 0.206 |
| $1/2S_{10}$ | 4 | 6.03 | | 2.56 | | 0.292 |
| $1/4S_{10}$ | 4 | 10.26 | | 5.79 | | 0.412 |
| Hermes | 6 | 12.01 | | 8.54 | | 0.935 |
| Tarball | 6 | 10.01 | | 6.54 | | 0.517 |
| Orion 4800 | 6 | 8.35 | | 4.88 | | 0.392 |
| Orion Tracker | 8 | 8.08 | | 4.61 | | 0.897 |
| Nova Tech | 7 | 6.13 | | 2.66 | | 0.311 |

* using S-X and S-$S_{10}$ data

## 4. FIELD TRIALS and ERROR ANALYSIS

The Bedford Basin, where most of the field trials were conducted, has a central area approximately 3 km by 4 km, with a tidal-narrows at the south end about ½ km wide. Surrounding hills are of similar low profile to give a uniform wind field across the Basin. The field program documented by White et al. (2016) consists of over 40 field trials. The report includes plotted positions, plotted wind speed, plotted buoy speeds, and tabulated average wind and buoy speeds. Figure 3 is an example of the plotted positions.

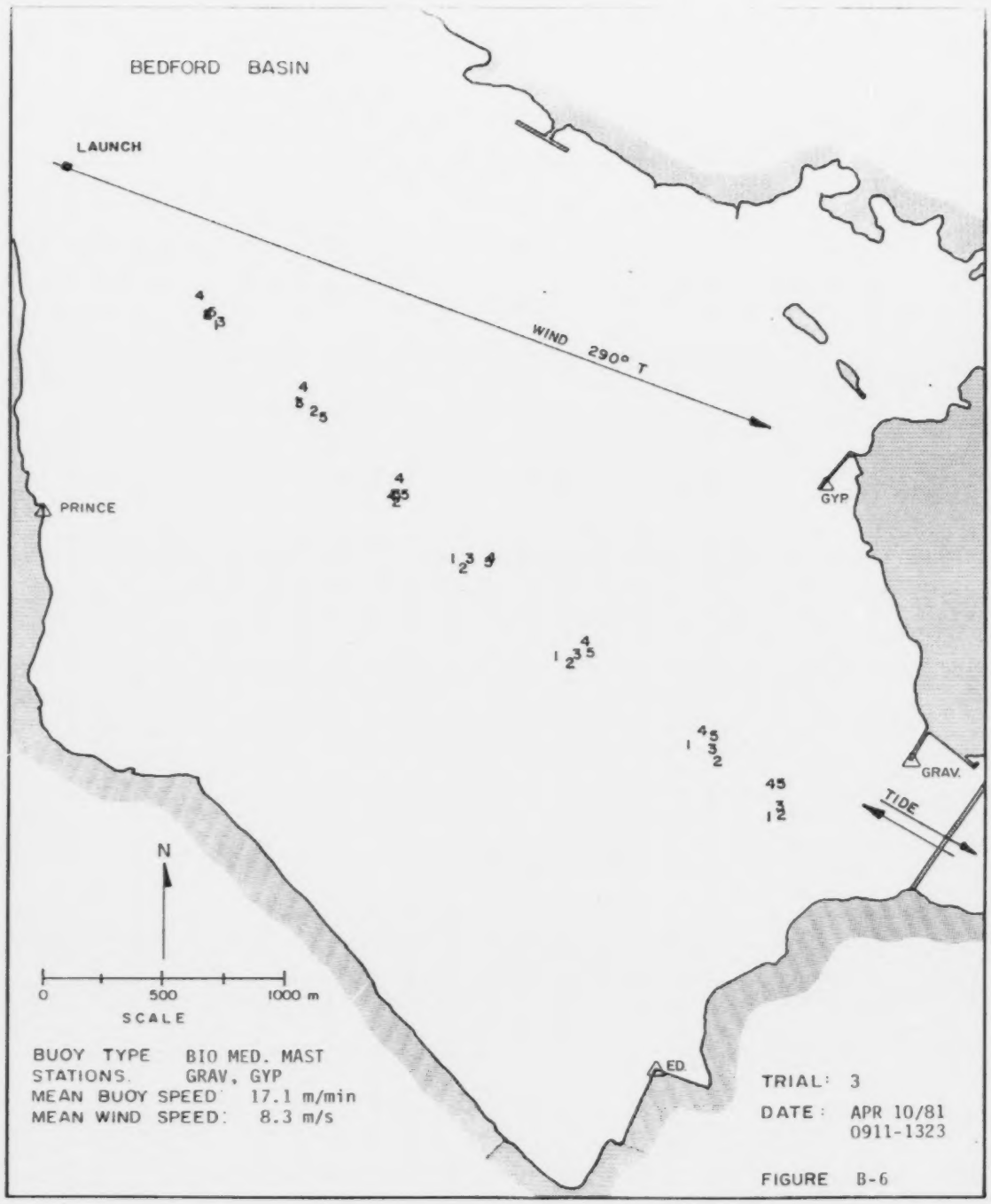


Figure 3: Plan view of the Bedford Basin with plotted results from Trial 3. Five identifiable M type buoys are tracked. Fixes are relative to two of the shore stations: Prince, Gyp, Grav, Ed.

A typical trial consisted of 5 identical buoys for each type, deployed simultaneously, and tracked over a period of up to 4 hours. Fixing the location was done by the near shore position fixing technique 'Mini-Ranger' installed on the work boat. Typically 3 or more fixes of location were made. The work boat, while attempting to not disturb the drifters, moved down wind after each set of fixes and waited for the buoys to pass by. Repositioning to the side of each buoy for a new fix is estimated to be accurate to at least ± 7m. The shore reference stations are shown in Figure 3, see Elliott and Fowler (2018) for details. Based on the quoted 'Mini-Ranger' error of ± 2 m and boat positioning relative to the buoys of ± 7m, the overall position error for a fix is about ±9 m.

The trials were planned for wind speeds over 5 m/s with a weather pattern stable over many hours. Wind speed was recorded on the work boat at 10 m height using a calibrated (±1%) cup anemometer. From experience with cup anemometers we can expect that this application on a moving boat to be reliable (e.g. Busch et al. 1980, 'Problems of overspeeding and angular response notwithstanding, well designed and calibrated cup anemometers are typically accurate to within ±1% of the actual reading above 5 m $s^{-1}$'). However, given the reality of a tall mast on a shifting platform, the estimated accuracy of wind speed would be the ± 0.5 m/s stated in White et al. (1983). For the data, which are in the range 5 m/s to 10 m/s, this means at least 5% to 10% accuracy. The bulk of the data were collected sufficiently down wind of the shore to expect the wind profile, U(y), of the boundary layer over the Basin to be that for the local sea surface drag coefficient, and therefore a near constant log profile for a given wind speed.

To get the separation velocity, $\Delta v$, we need the average $\Delta d_i$ and $\Delta t_i$ of the two groups (typically 5 of each) of paired buoy types. There is no fixed error estimate for the $\Delta v$, it being dependant on the $\Delta d_i$ and $\Delta t_i$ of a given trial. The field data range from a $\Delta d$ of 1 km to 4 km, and $\Delta t$ of 1.5 hours to 4 hours. As stated above the estimated position accuracy is worst case ±9 m. The time of a position fix is given as ±1 min. Two time measurements and two positions are needed for a given $V_i$. The $\Delta v$ estimate needs data for two groups of buoys each with an expected accuracy limitation of ±2 min and ±18 m (the error for an individual buoy and for the mean of a cluster is taken to be the same).

Here are examples of worst case errors (wce) for $\Delta v$ with these limitations. It is assumed that the drift rate will be 3% $U_{10}$.

- at 5 m/s wind for 2 h the wce is ±0.6 m/min.

- at 10 m/s wind for 2 h the wce is ±0.9 m/min.

- at 5m/s and 10 m/s wind for 3 h the wce is ±0.4 m/min.

Data for high winds and short times are the least accurate: for one hour at 10 m/s the wce is ±1.80 m/min. The intent is to have accuracies near the ±1 cm/s or ±0.6 m/min stated for ADCPs. Initial analysis showed this expected high scatter. Thus, for given pairs, speeds were calculated using the longest duration averages of quality data available. The multiple fixes taken during the trials were used to evaluate and to ensure data quality; this is given in detail in Elliott and Fowler (2018). However, for some data only available with the $S_{10}$ buoy as reference (these data are for the non-BIO Barrel Drifter part), the averages of individual segments are used. The overall averages do not change significantly, but the scatter will be larger. This allowed for adjusting to any significant wind changes.

Following is the analysis detail for the various pair combinations, with results shown in Table 2. For each trial of a pairing there is a separation velocity, $\Delta v$, at a measured mean wind speed, $U_{10}$. All trials for a given pairing are presented as a scatter plot as $\Delta v$ vs $U_{10}$ fitted with a least square line. These plots are given in Appendix 1.

5. DRIFT SPEED for X, S, M, and L

Referring to Table 2, column 1, Buoy Types X, S, M and L were deployed to evaluate the different drift rates resulting from a change in diameter of the mast/antenna on the BIO Barrel Drifter. For all (forty-six) trials the S type buoy was chosen to be the reference buoy deployed in every trial to ensure that comparative data would be available. Seven trials (25, 26, 27, 28, 44, 45, & 46) were selected for which the drift pattern was consistent over the duration, and shoreline or tidal affects appeared to be at a minimum. As an example, Figure 4 (and A2), shows the speed of the M buoys relative to S type (all at 20 or 30 kg ballast). A similar plot for the L type, Figure A1, is in Appendix 1. Insufficient data were collected to compare the X type with S type at the heavier ballast, however a second group of five trials (21, 22, 23, 24, & 29) using the S type ($S_{10}$) at 10 kg with X type ($X_{10}$) at 10 kg are considered a good substitute, Figure A3, Appendix 1. The scatter of the data in all three comparisons is about that expected for 'worst

case experimental error'. Figure 4 shows a typical error bar: Δv of ± 0.6 m/min and for $U_{10}$, ± 0.5 m/sec.

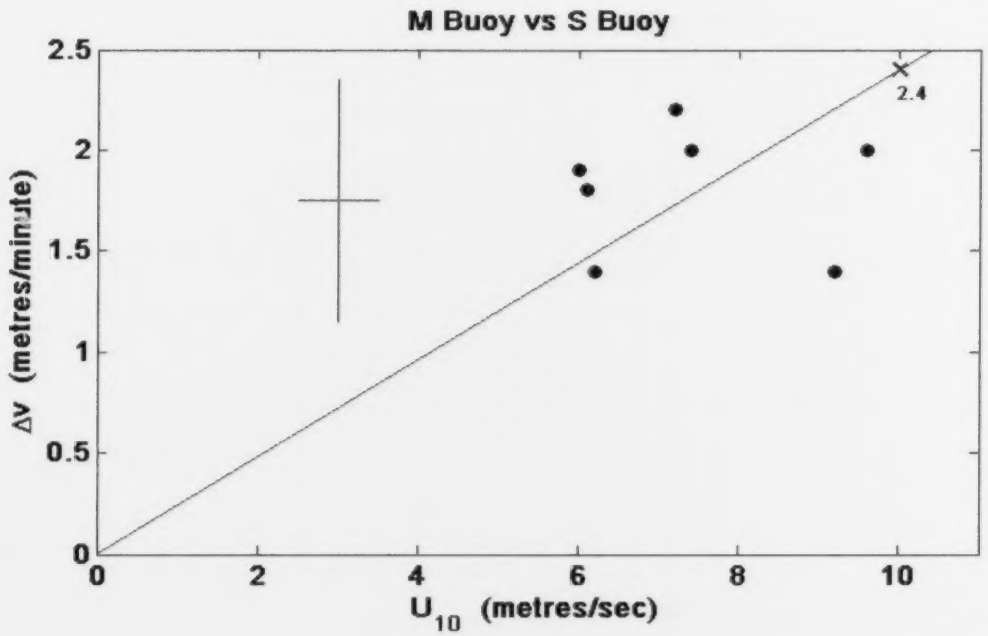


Figure 4: Plot of average speed of separation Δv between reference buoy S and M as a function of wind speed $U_{10}$. An X labeled 2.4 is the mean Δv at 10 m/s. Each dot plotted is an average of up to 5 buoys of each type. Shown to the left are potential error bars: ±0.6 m/min and ±0.5 m/s. Note that each trial (dot) has a different worst-case error for Δv, dependant on the time elapsed and distance traveled. Also plotted is a least square line, forced to pass through zero. See text for detail.

Based on the predicted near constant drag coefficients, there would be a linear relationship between Δv and $U_{10}$. These graphs, Figure 4 and Figures A1, A2, and A3 (Appendix 1) show a least square line forced to pass through zero. The data have high scatter, however there is no pattern to suggest that a linear fit is not appropriate, see Appendix 1. For reference the symbol 'x' is plotted on the least square line at 10 m/s. The same style applies to the other data shown in Appendix 1. The drift rates projected at 10 m/s from Figures A1, A2, and A3 (marked as an 'x') are used for Figure 5.

Figure 5 shows the incremental drift speeds $\Delta v$ for the four buoy types as a function of $\{A_a/A_o\}^{1/2}$. Also shown is a least square line. Although no data were available to plot a value for X in these trials, the $\Delta v$ value from the pair $S_{10}$ : $X_{10}$ plotted in Figure 5 agrees with the least square line projection. This suggests that although the lighter ballast pair had slightly higher mean drift speed, the separation velocity was not measurably different. The close agreement from all four types of configurations of the BIO Barrel buoy shown by Figure 5 gives confidence that the near linear drag balance formulation used is a good estimate of antenna drag error on an X type buoy.

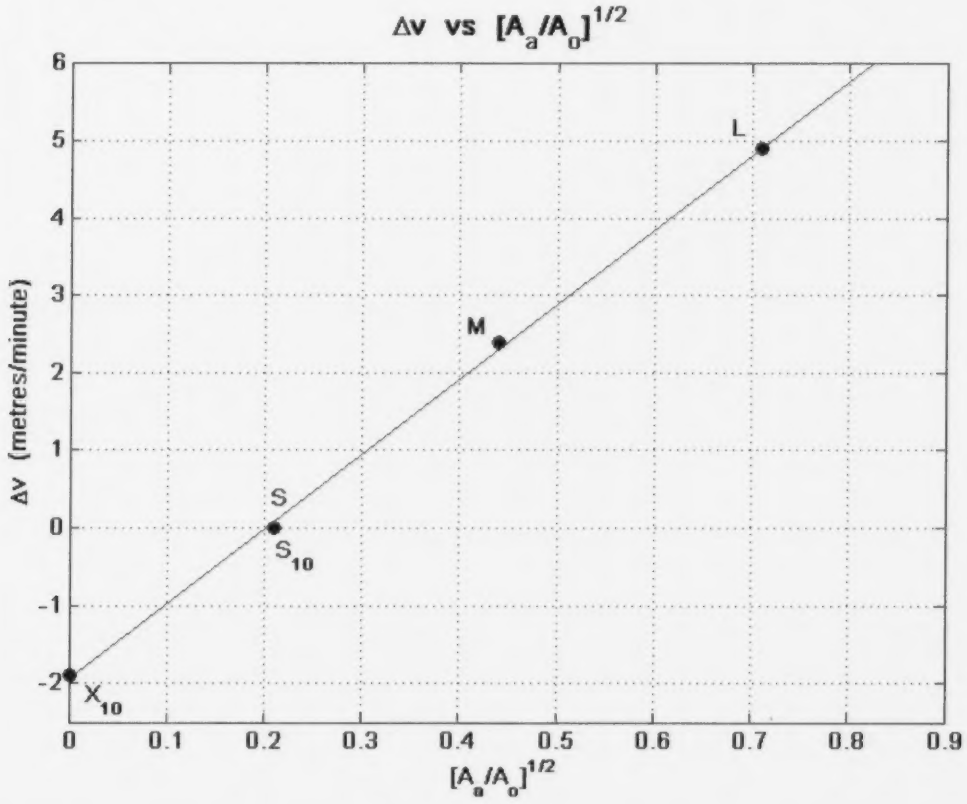


Figure 5: Plotted as a function of the normalized antenna area are the separation speeds $\Delta v$ m/min at wind speed of 10 m/s for each of the buoy types, using values from Figures A1, A2, and A3. The solid line is a least square line.

There will always be some uncertainty as to what Lagrangian current an X type buoy represents given that there can be a shear in the current. Drag on the barrel, for modest, near linear shear, should balance vertical differences to follow the current at about mid-depth, i.e. about 40 cm depth. For wind driven currents with wave breaking, the shear would likely be, if anything, higher in the upper 40 cm. Thus, the drift observed would be representative of a mean current near but above 40 cm.

As noted in Section 2, the barrel 'X' was adjusted to have a freeboard of 2 cm. An estimate of the potential drift speed of the X drogue from wind drag can be made using the same formulation as above. Drag coefficient $C_o$ for the barrel is about 0.75, based on it being a symmetrical half of a finite circular cylinder with length of 5 diameters. The coefficient $C_a$ for the in-air portion can only be approximated; the coefficient value for an airfoil (aspect ratio 6) of 0.02 is used (an upper limit would be 0.06, the value for an infinite tilted (streamlined) cylinder. Wind speed for a $U_{10}$ of 10 m/s has a value about 3 m/s at 1 cm. The estimated X drift from the freeboard is about 0.18 cm/s. This 'freeboard' effect will of course be less at lower wind speeds.

Figure 6 is a plot, against wind speed, of the shore-referenced currents observed by the M Buoy in the Bedford Basin. Note that these observations include all residual and oncoming tidal flows as well as the wind driven currents of the hour, the reason for the scatter. Shown as a solid line with a label 'observed' is a least square line for the observed drift speed and forced to pass through zero. For reference purposes the 2% and 3% of wind speed lines are also shown. The line with label 'w antenna correction' is the adjustment for the antenna drag using Figure 5. The M Buoy had an observed average speed of about 3.1% $U_{10}$; an X buoy, based on the correction given in Table 2, would have had an average speed of about 2.4% of $U_{10}$, i.e., antenna drag is about 0.7% $U_{10}$. A note of caution here. Although these results agree closely with the 'rule of thumb' of oil drift being 3% $U_{10}$, these wind-driven drift measurements are for a partially enclosed basin.

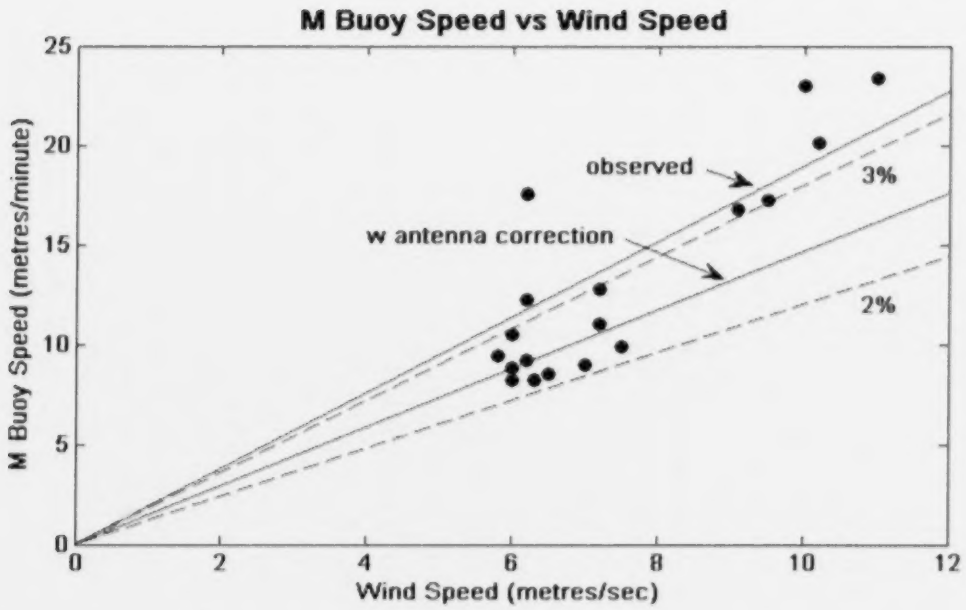


Figure 6: Plot of the shore-referenced drift speeds observed for the M Buoy. The solid line labelled 'observed' is a least square line fit. The 'w antenna correction' is the adjustment for antenna drag. Also shown are 2% and 3% $U_{10}$ wind speed.

6. DRIFT SPEED for S, ½ S, ½ M, and ½ L

The next set of buoys that were paired are S, ½ S, ½ M, and ½ L, see Table 2 and Figure 1. Data were collected with a set of drifters similar to the above full depth barrel type, but with a barrel of one-half the depth, i.e. about 40 cm depth, all identical. The antennas were the same as S, M, and L, Table 1. The S buoy, full depth, was the reference, and all were ballasted to 20 kg. Five trials (36-40) were conducted. Figures A4, and A5, Appendix 1, are scatter plots of observed $\Delta v$ for the pairs: ½ M : ½ S and ½ L : ½ S. The $\Delta v$ from the least square line projection to 10 m/s in Figures A4 and A5 are plotted in Figure 7.

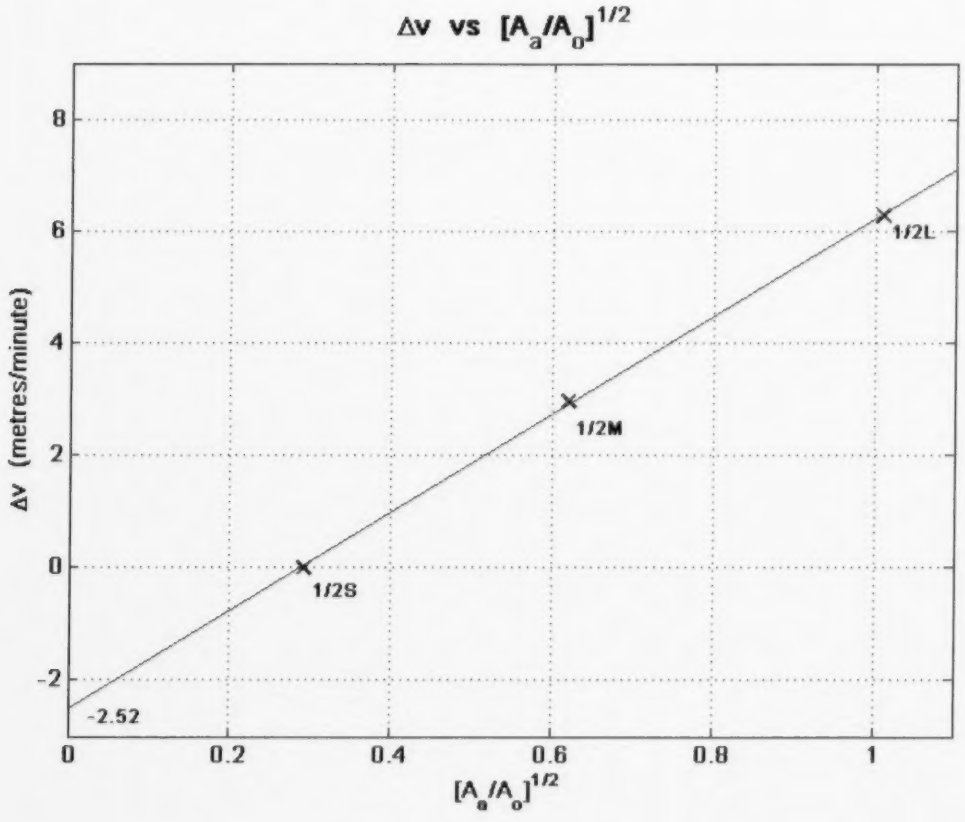


Figure 7: Shown is a plot of the separation speed Δv between the reference buoy ½ S = 0 and ½M and ½ L, as a function of $[A_a/A_o]^{1/2}$. At $[A_a/A_o]^{1/2}$=0 is a projection by a least square line to -2.52 m/min.

The least square line projection to no-antenna or a hypothetical ½ X (not included in this study) is -2.52 m/min. Figure A6, a scatter plot in Appendix 1, gives the Δv speed between S and ½ S at 10 m/s, as 2.69 m/min. Knowing the Δv between S and X as 1.94 m/min (above), between S and ½ S as 2.69 m/min, and between ½ S and projected ½ X as 2.52 m/min, the speed of a ½ X (half-barrel) on average would be 2.1 m/min faster than a X (full-barrel). The half-barrel would be a mean current averaged over the top 40 cm.

The full-barrel and half-barrel buoys were not deployed together so a comparison of their relative drift speeds is not rigorous, that is, one cannot assume that similar winds produced the same vertical shears. However, the measured difference is worth a comparison. Assuming linear shear with the mid depth of the barrel as the appropriate level for the measured speed, there is an estimated 2.1 m/min speed difference across 20 cm. Or, an 8 m/min (13.6 cm/s) difference between the top and the bottom of the BIO Drifter. Taking 3% of a 10 m/s wind, i.e., 30 cm/s, as a typical 'surface' velocity, linear shear from that surface speed would imply an approximately 2 m 'mixed layer depth' with uniform linear shear. One cannot expect the profile to be this simple given active mixing from wave breaking (spilling) effects at the surface, however these are reasonable numbers. At this linear shear, the M buoy would have a speed about the same as the surface velocity: Figure 6. By co-incidence, antenna induced wind drift $\Delta v$ for the M buoy is about equal to the projected linear shear between the surface and 40 cm depth, i.e., X buoy.

## 7. DRIFT SPEED of S and $S_{10}$

As noted above, a common S type buoy was used throughout. However, a change in the ballasting was made for design reasons and, as a result, there were two versions (see Table 2): S and $S_{10}$. A cross-calibration is needed between the two 'standards'. Figure A7, Appendix 1, is the scatter plot, showing a mean $\Delta v$ of 1.53 m/min, S slower than $S_{10}$. In Figure 6, a comparison of the drift rate of the M Buoy relative to the wind speed gave a best fit slightly above 3% of the wind speed $U_{10}$. Better statistics can be obtained by using the combined data collected with both reference buoys, S and $S_{10}$, since together they cover the entire data set (with some overlap). Shown in Figures A8 and A9, Appendix 1, are the comparisons between wind speed and buoy speed for 17 trials that used S and 25 trials that used $S_{10}$. At 10 m/s the least square line fit gives values of 19.0 and 16.9 m/min respectively. For comparison, 3% of 10 m/s is 18 m/min. Adjusting the drift rate of each buoy to the X reference and using a weighted average, gives an X buoy speed of about 2.53% $U_{10}$. This places the M buoy at about 3.25% $U_{10}$. This value is slightly higher than the 3.1% shown by Figure 6. Given that the data shown in Figures A8 and A9 are highly scattered and the M type is the design for the BIO Barrel Drifter, the Figure 6 results are preferred for following comparisons.

8. DRIFT SPEED of $S_{10}$ with ½ $S_{10}$ and ¼ $S_{10}$.

Next in Table 2 are the two types called ½ $S_{10}$ and ¼ $S_{10}$. They are variants on the standard full-barrel, as a half-barrel and a one-quarter barrel, evaluated using the $S_{10}$ as reference. Figures A10 and A11, Appendix 1, are the scatter diagrams. These trials were intended to explore the sensitivity of the depth of the in-water portion of the BIO barrel. The data show that the ratios between $[A_a/A_o]^{1/2}$ and $\Delta v$ have a significantly higher $\Delta v$ than required if they were to follow the simple model used above. The likely reason is that the in-water drag coefficient $C_o$ has not remained constant. Given their shape, the half-barrel and quarter-barrel are probably responding dynamically more as a hemisphere than a portion of an infinite cylinder. With such a different shape, the coefficient would be significantly different (Daugherty and Ingersoll 1954). The change in $\Delta v$ from $S_{10}$ to ½ $S_{10}$ to ¼ $S_{10}$ is however well defined, shown below in Figure 8. This gives added confidence in the repeatability of the patterns observed and ability to adjust design parameters. The full depth BIO barrel may also not strictly mimic a portion of a finite cylinder, however it was only required the $C_o$ remain constant for all four antenna types, as planned.

9. DRIFT SPEED of OTHER BUOYS

The final entries in Table 2 are five add-ons to compare with the BIO Barrel Drifter. Tarball is a BIO Depot (technical staff) entry; the others are commercial products, with three marketed as oil spill trackers. Inter-comparison of the commercial products was lacking, and these entries were done with the full collaboration and in-kind support from industry. A more detailed schematic profile and some measured parameters for these drifters is given in Elliott and Fowler (2018). Their respective scatter plots are in Appendix 1 as Figures A12 through to A16. Table 2 lists the observed $\Delta v$; their reference was $S_{10}$. For this group with $S_{10}$ as reference, shorter time lapse data were used to allow for additional editing. As a result there is higher scatter. Also given in Table 2 is a transfer of these speeds to an X reference through the X to $S_{10}$ comparison. Results are plotted in Figure 8.

## 10. COMPOSITE of BEDFORD BASIN TRIALS

For comparison, all $\Delta v$ values in Table 2 are plotted in Figure 8. These are the $\Delta v$ expected at a $U_{10}$ of 10 m/s. Figure 8 has two components. First, the plot shows for each pairing the separation velocity $\Delta v$, with X buoy as reference, as a function of their drag area profile $\{A_a/A_o\}^{1/2}$. The second component is a series of dashed lines parallel to the $\{A_a/A_o\}^{1/2}$ axes. These are the 'best guess' values for the speed of the buoys relative to $U_{10}$ over Bedford Basin, based on Figure 6, and estimated to be accurate to about $\pm 0.1\%$ $U_{10}$. For example, the drift speed of the buoy M is approximately 3.1% $U_{10}$.

The consistent patterns in the BIO Barrel data, as illustrated in Figure 8, give confidence in the overall results:

-The points S, M, L and X, and separately, ½ S, ½ M, and ½ L, are well connected by a least square line, see Figures 5 and 7 above.

-The difference in $\Delta v$ between these two lines, 2.1 metres/minute at $\{A_a/A_o\}^{1/2} = 0$, can be interpreted as the difference in mean velocity at 40 cm depth (X), compared with a mean at 20 cm depth (½ X). With the best guess for the speed of X as 2.4% of $U_{10}$, adding the observed shear (4.2 m/min over 40 cm) to the X drifter speed gives a surface velocity of 3.1% $U_{10}$. A reasonable value.

-There is also the linear pattern, connected by a least square fit, to the group $S_{10}$, ½ $S_{10}$, and ¼ $S_{10}$.

-The $\Delta v$ between $S_{10}$ and ½ $S_{10}$, 2.56 m/min, is close to that for S and ½ S, 2.69 m/min.

-Likewise the projection of S, M, and L to X, was duplicated by $S_{10}$ to $X_{10}$.

All suggest there is a $\Delta v$ accuracy of about $\pm 0.1$ metres/minute.

Five other buoys are shown as individual points in Figure 8.

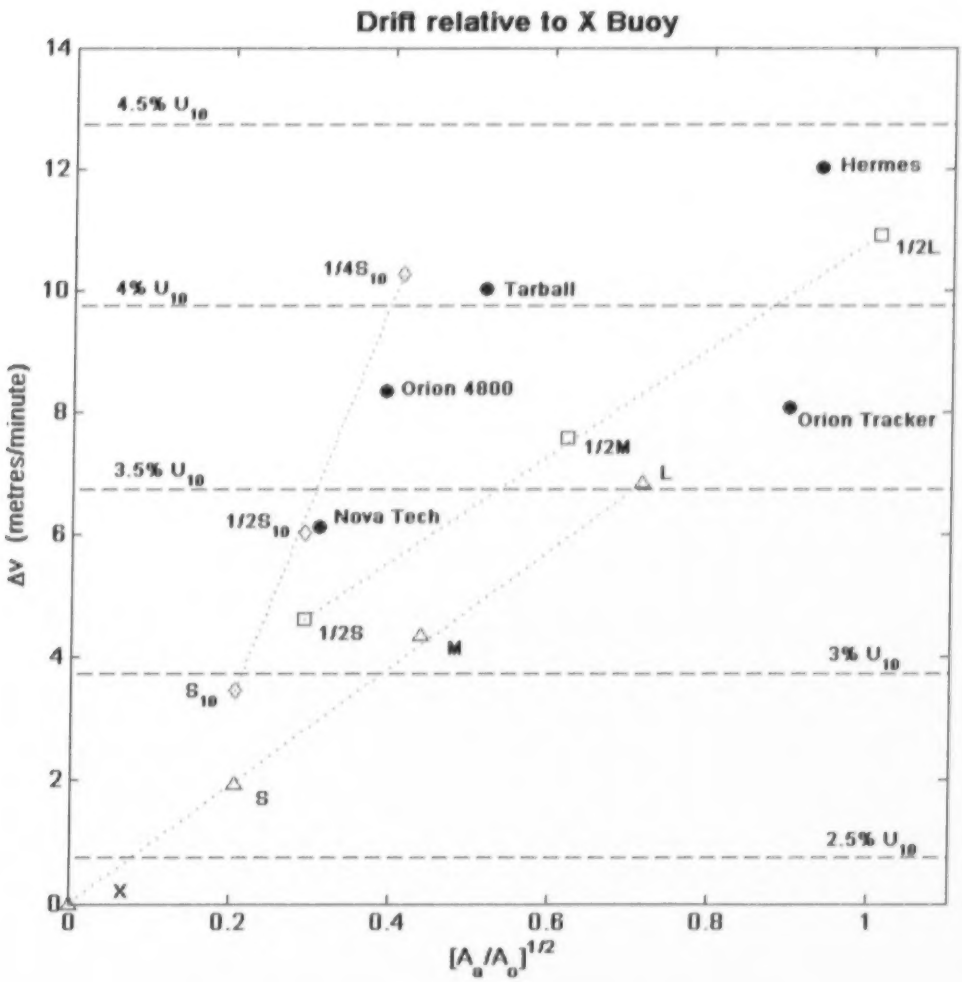


Figure 8: A composite of the buoy types showing the relative separation speed, $\Delta v$, at 10 m/s as a function of $[A_a/A_o]^{1/2}$. All have been adjusted to the common reference X, see Table 2. Also shown, as dashed lines, is a best guess estimate of their total speed as a percentage of wind speed $U_{10}$. The dotted least square lines connect those buoys combined to show dependence on the design parameters of mast/antenna diameter, barrel depth, and ballast.

The Hermes Buoy was developed for deployment in the Southern Ocean to monitor temperatures and air pressure as part of the international program GARP (late 70s). It is of similar proportions to the L Buoy type; with higher wind/wave profile it can be expected to have higher drift rate.

Tarball is of a design similar to the floats used by east coast in-shore fishers to keep track of gear. It was added out of curiosity since they are sometimes seen as opportunistic drifters. It is shown to be a fast drifter.

Orion 4800 and Orion Tracker are (were) commercial products intended for tacking an oil spill. Both showed drifts significantly above 3% wind speed. Neither can be considered as a good representation for a mean current of the top metre.

Nova Tech, also a commercial product, has a drift rate about 3.4% wind speed. This design, intended as an air deployable tracker, is based on studies conducted by Ages (1982). His limited field and laboratory trials indicated a value of about 2% $U_{10}$ for drift rate. This more detailed field evaluation was part of his recommendations for further work.

## 11. DRIFT SPEED in OCEAN TRIALS

On two occasions buoys were deployed off the mouth of Halifax Harbour. The first, on November 18, 1982, included 6 each of 4 types: $X_{10}$, $S_{10}$, $M_{10}$, and $L_{10}$. Wind speed of 6.5 m/s was measured by the deploying ship's anemometer. Spatial separation was monitored by helicopter overflights flying a mosaic pattern of photographs– this technique had been tested in Bedford Basin (see Elliott and Fowler 2018). Figure 9 is a plot of separation velocity. The $\Delta v$ pattern experienced in the Bedford Basin is repeated for these data, and with similar accuracy. The accuracy of the wind speed and the separation velocity – estimated by using the deployment ship as scale – are not as well-known as for the Basin data, however the values measured fall within the scatter plot of data from the Basin. When comparing Figure 9 with similar data from the Bedford Basin (e.g., Figure 5), note that the offshore data are for approximately 6.5 m/s, not 10 m/s.

The second occasion was the deployment of six S type in an oil slick, a small spill planned as part of an experiment on dispersants. In 1983, on September 12, 16, and 17, the buoys were monitored for 2, 2½, and 3½ h. Throughout they maintained their relative position within the slick pattern as shown in a sketch from aerial photos. This was a limited test of tracking given the short duration and light winds (10 km/h to 18 km/h). See Elliott and Fowler (2018) for more detail.

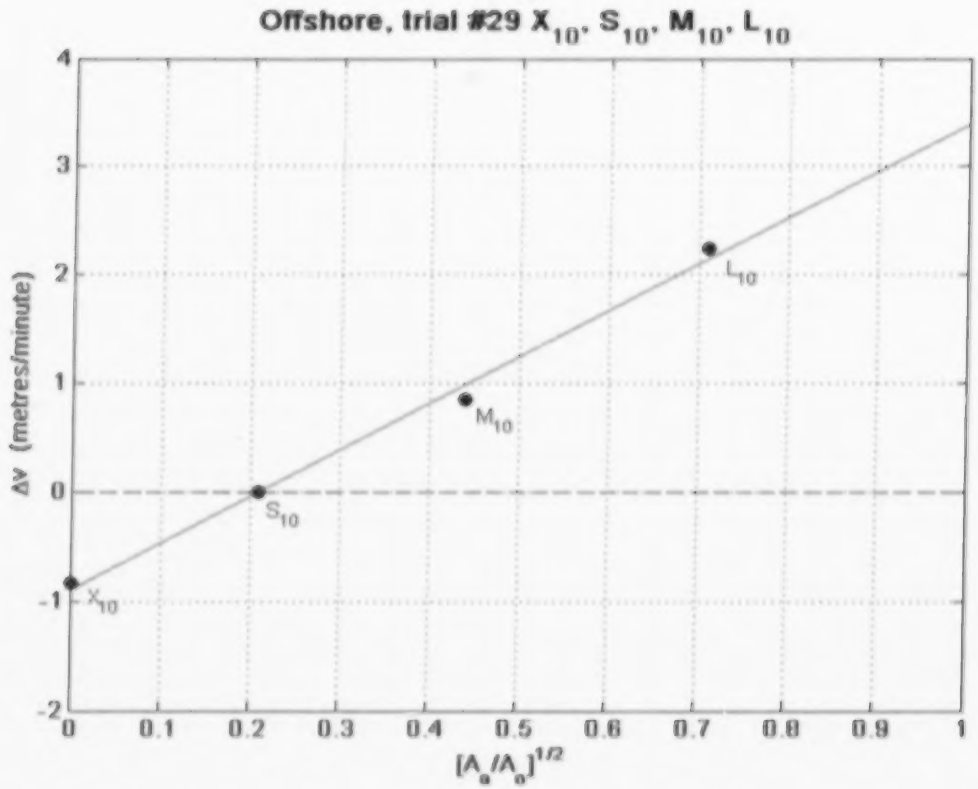


Figure 9: Results from a single trial offshore the mouth of Halifax Harbour. There were 6 buoys of each of the 4 types and all are the lighter ballast $S_{10}$ variety. Data were analyzed from aerial photographs as separation rate relative to the $S_{10}$ buoy. The solid line is a least square line. Wind speed recorded from the accompanying ship anemometer was estimated to be 6.5 m/s. See text for details.

## 12. CONCLUSIONS

The development and field trials of the BIO Barrel Drifter were as successful as could be expected. The objective was to build confidence in a Lagrangian drifter through studies in an open ocean environment. In the early 80's a number of different drifter designs were in use, based mainly on laboratory studies, see e.g. Vachon (1980). Each served their application, but their tracking performances and inter-comparisons in an open ocean environment were lacking. Figure 8 has examples of the then state-of-the-art commercial products. The original planning for the BIO Barrel Drifter had the concept of a simple design and construction capable of being

modified easily to test ideas for 'desirable' Lagrangian behaviour. This report is the documentation of what was planned as Phase 1, an examination of the influence of the above water component (mast/antenna) on the behaviour of the under-water drogue. The results documented here were sufficiently encouraging to users that the M type became the design for a commercial product based largely on the close agreement with then existing studies on oil drift. Further phases with field comparisons examining with how well the 'X' drogue tracked oil slicks and oil particles, floating objects, biota, etc., began, but changing priorities postponed the program (see Section 11 above). That opportunity continues.

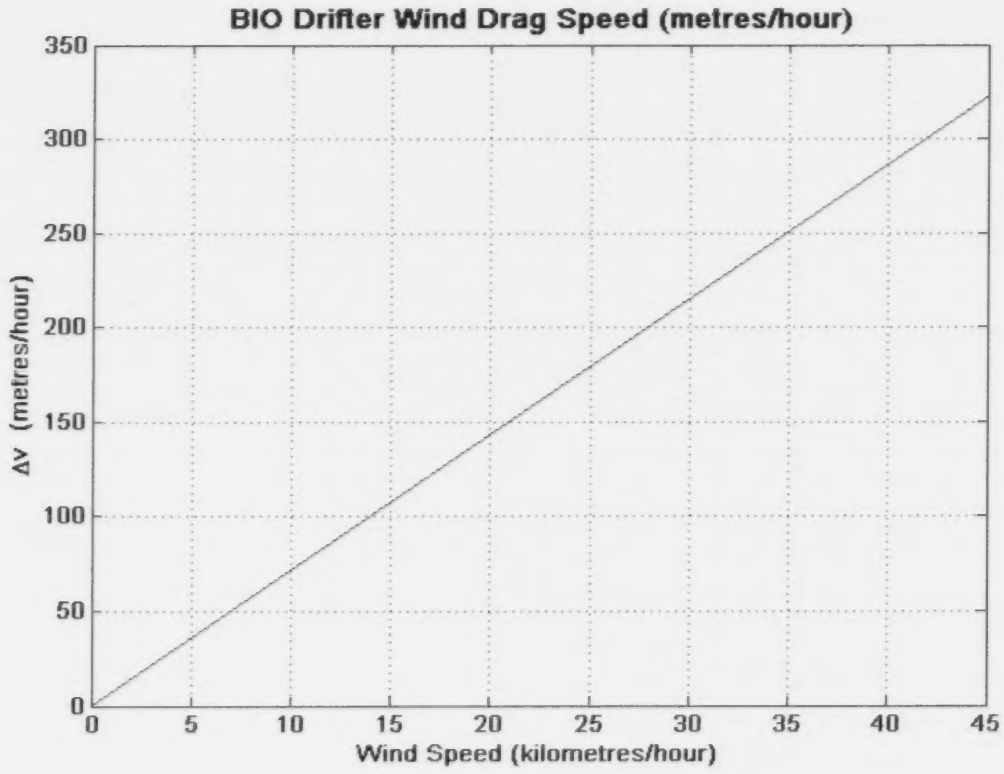


Figure 10: A quick reference plot of the 'wind-drag' drift velocity, $\Delta v$ (m/h), for the BIO Barrel Drifter (M Buoy) as a function of wind speed (km/h). The line is $\Delta v = 7.22U_{10}$. The buoy is drifting at 1 cm/s relative to the 'mean current' for a wind of 5 km/h

With the results provided by this data set, BIO Barrel Drifter drift speed with antenna can be corrected to remove the influence of antenna drag to an accuracy of about, or better than, ±1 cm/s. With improved accuracy from the antenna correction and with some confidence in what bulk current is being measured this drifter is suitable for use as a supplement to moored current metre data and for calibration of numerical models.

For quick reference, Figure 10 shows the antenna correction $\Delta v$ (m/h) plotted against wind speed $U_{10}$ (km/h) at 10 m height. As with the forgoing analysis the near linear relationship is use. Expressed as a formula the correction is $\Delta v$ (m/h) = 26.0 $U_{10}$ (m/s), or $\Delta v$ (m/h) = 7.22 $U_{10}$ (km/h). As shown by Figure 10, a wind above 5 km/h gives an expected increase in drift above 36 m/h or 1 cm/s. The success of this study was challenged by field sampling error as shown by Figure 4 and by the scatter plots in the Appendix. Obtaining 'good' deployment and recovery times and positions is important. Proper ballasting was needed to avoid unwanted tilting of the antenna and excessive heave response of the drogue (barrel). Even a modest tilt, e.g. 45°, will reduce the drag coefficient of the antenna by a factor of 10. Given the very dynamic and non-linear nature of the air/sea interface, caution should be used in extending these results to higher wind speeds.

## 13. REFERENCES

Ages, A.B. 1982. The development of an oilspill tracking technique. Can. Tech. Rep. Hydrogr. Ocean Sci. 8: vi + 29p.

Busch, N.E., Christensen, O., Kristensen, L., Lading, L., and Larsen, S.E. 1980. Cups, vanes, Propellers, and Laser Anemometers. *In* Air-Sea Interaction Instruments and Methods. Eds. F. Dobson, L. Hasse, and R. Davis. Plenum Press. N.Y.

Drozdowski, A., Horne, E., and Page, F. 2018. Hydrographic measurements near the greater Port Hawkesbury area. Can. Tech. Rep. Fish. Aquat. Sci. 29XX: viii + ??p.

Elliott, J.A., and Fowler, G.A. 2018. Field Trials Observing Wind/Wave Drag on BIO Barrel Drifter and other Lagrangian Surface Drifters. Can. Data Rep. Fish. Aquat. Sci. 1283: v + 256p.

Forrester, W.D. 1971. Distribution of Suspended Oil Particles Following the Grounding of the Tanker Arrow. J. Mar. Res. 29, 2: 151-170.

Vachon, W.A. 1980. Drifters. *In* Air-Sea Interaction Instruments and Methods. Eds. F. Dobson, L. Hasse, and R. Davis. Plenum Press. N.Y.

White, W.D., Elliott J.A., and Lawrence D.J. 1983. Field Trials of Lagrangian Drifters for Tracking Oil. Unpublished manuscript. OERD Library, BIO Library, Dept. Fisheries and Oceans, Dartmouth, Nova Scotia.

## 14. APPENDIX 1

Scatter plots for the relative drift rate, $\Delta v$ (m/min), for each of the buoy pairs as a function of wind speed, $U_{10}$ (m/s). A least square line is forced to pass through zero. The mark 'X' on the line at 10 m/s, is labeled with the mean value for this buoy pair; this value appears in Table 2. Note that each value plotted is an average of up to 5 buoys of each type.

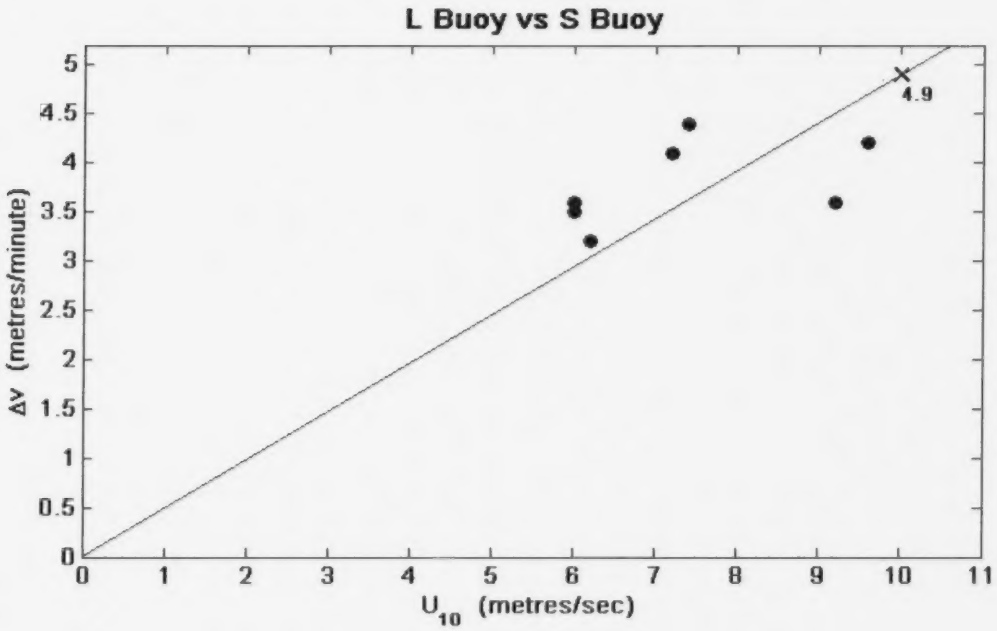


Figure A1: Scatter plot of the separation velocity, $\Delta v$, between the reference S and the buoy L as a function of wind speed, $U_{10}$. The solid line is a least square line. The data are for 7 trials.

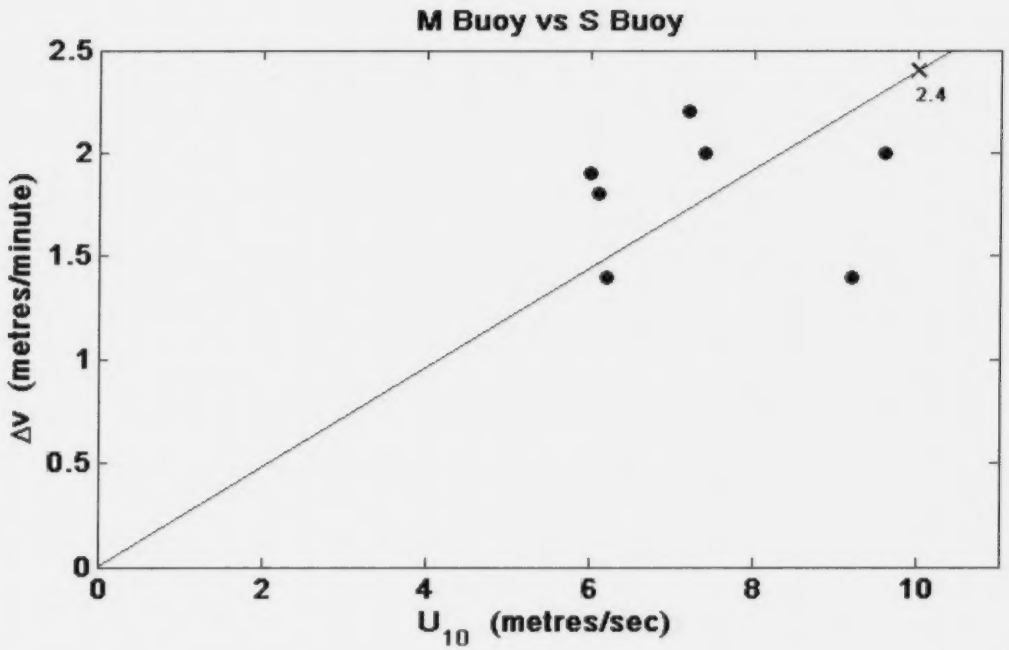


Figure A2: Scatter plot of observed separation speed, $\Delta v$, between the reference S and the buoy M as a function of wind speed, $U_{10}$. The solid line is a least square line. The data are for 7 trials.

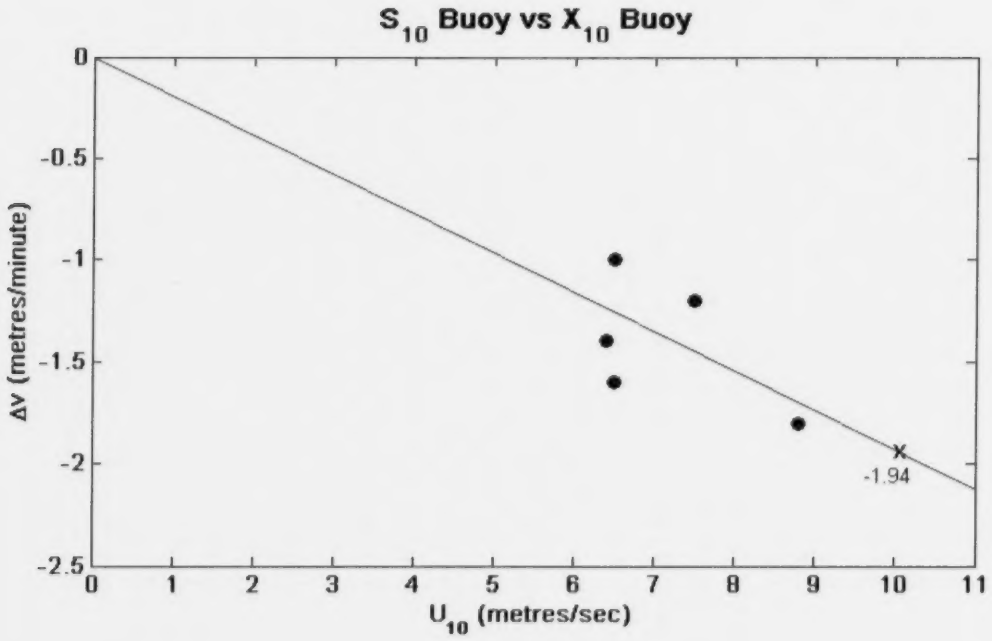


Figure A3: Plot of average speed of separation, $\Delta v$, between $S_{10}$ and $X_{10}$ as a function of wind speed $U_{10}$. Also plotted is a least square line, forced to pass through zero. Note that each value plotted is an average of up to 5 buoys of each type over 5 trials.

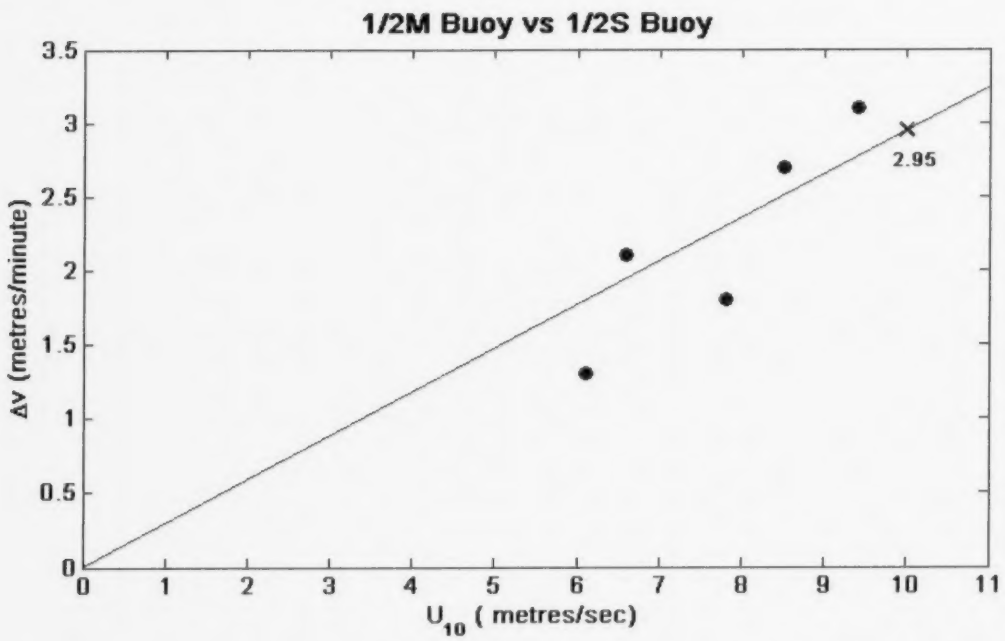


Figure A4: Plot of average speed of separation Δv between reference buoy 1/2S and 1/2M as a function of wind speed $U_{10}$. Also plotted is a least square line, forced to pass through zero. Note that each value plotted is an average of up to 5 buoys of each type.

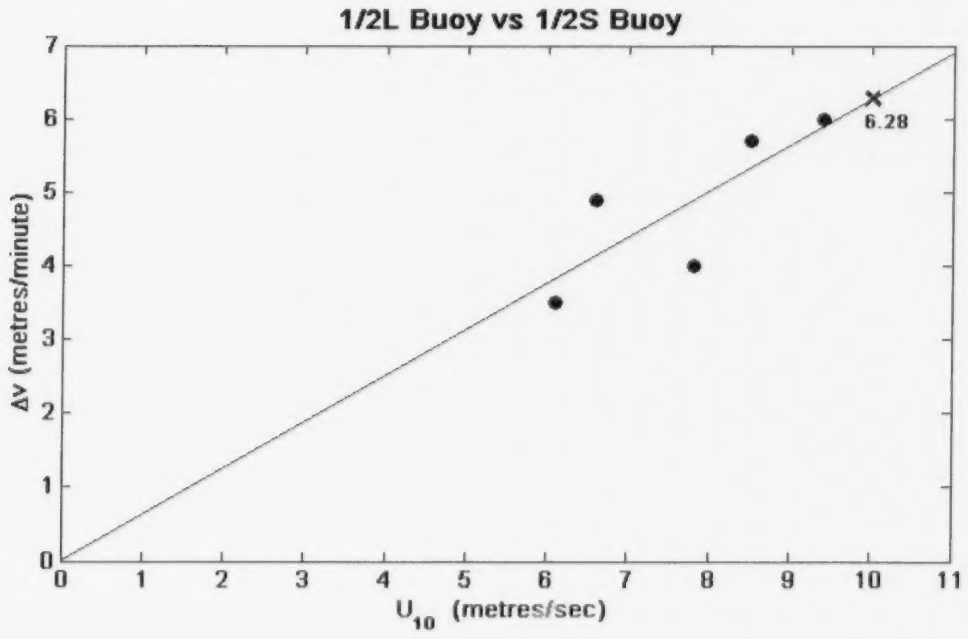


Figure A5: Plot of average speed of separation Δv between reference buoy 1/2S and 1/2L as a function of wind speed $U_{10}$. Also plotted is a least square line, forced to pass through zero. Note that each value plotted is an average of up to 5 buoys of each type.

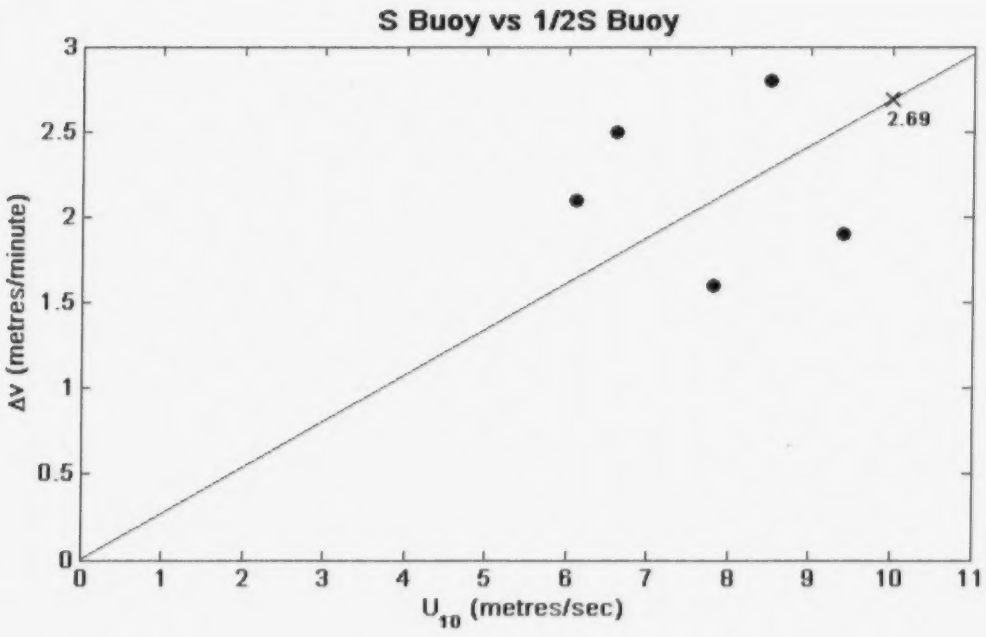


Figure A6: Plot of average speed of separation $\Delta v$ between reference buoy S and 1/2S as a function of wind speed $U_{10}$. Also plotted is a least square line, forced to pass through zero. Note that each value plotted is an average of up to 5 buoys of each type.

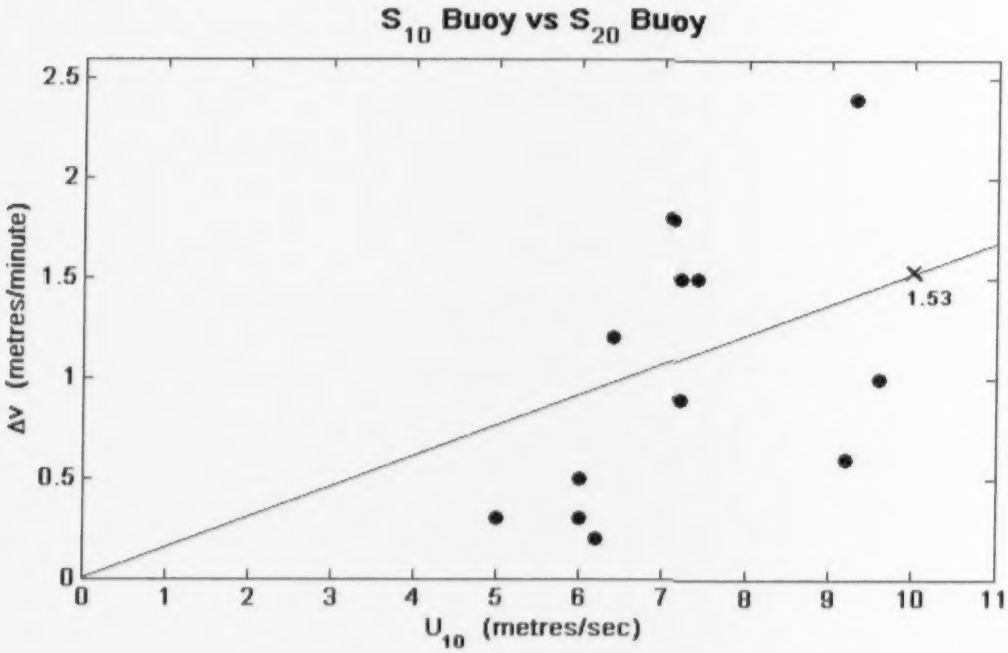


Figure A7: Scatter plot of the relative speeds, $\Delta v$, between the two S type buoys with different ballasts used for the reference buoy, $S_{10}$ and S. The apparent high scatter is due to the scale for $\Delta v$. See Figure 4b for example of potential error bars.

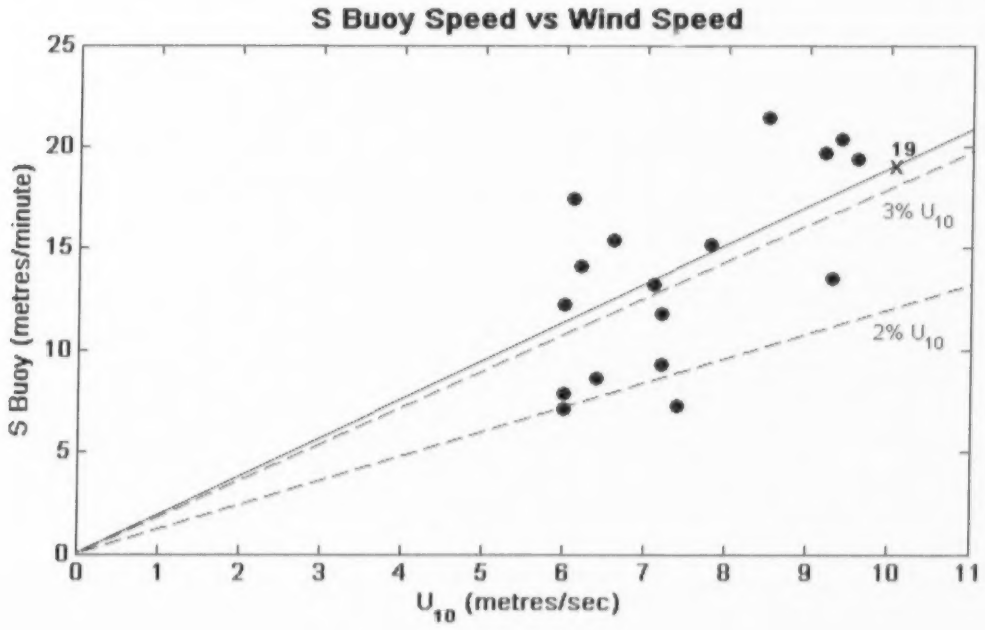


Figure A8: Scatter plot of the land referenced speed of the S buoy as a function of wind speed. A solid line is a least square line, the dashed lines as for the speed of 3% and 2% of $U_{10}$.

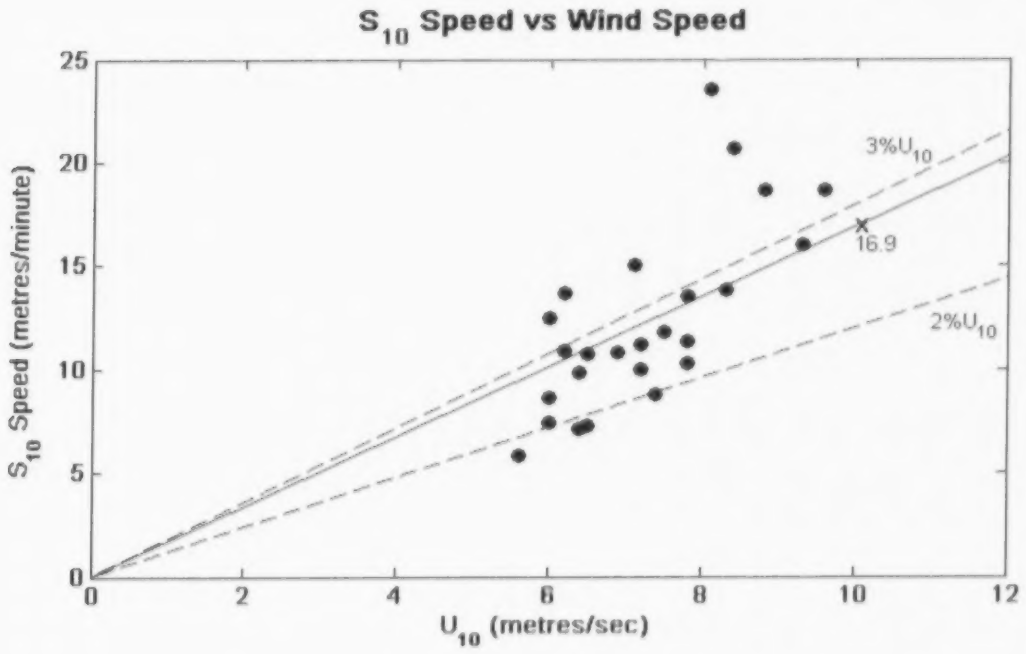


Figure A9: Scatter plot of the land referenced speed of the $S_{10}$ buoy as a function of wind speed. A solid line is a least square line, the dashed lines as for the speed of 3% and 2% of $U_{10}$.

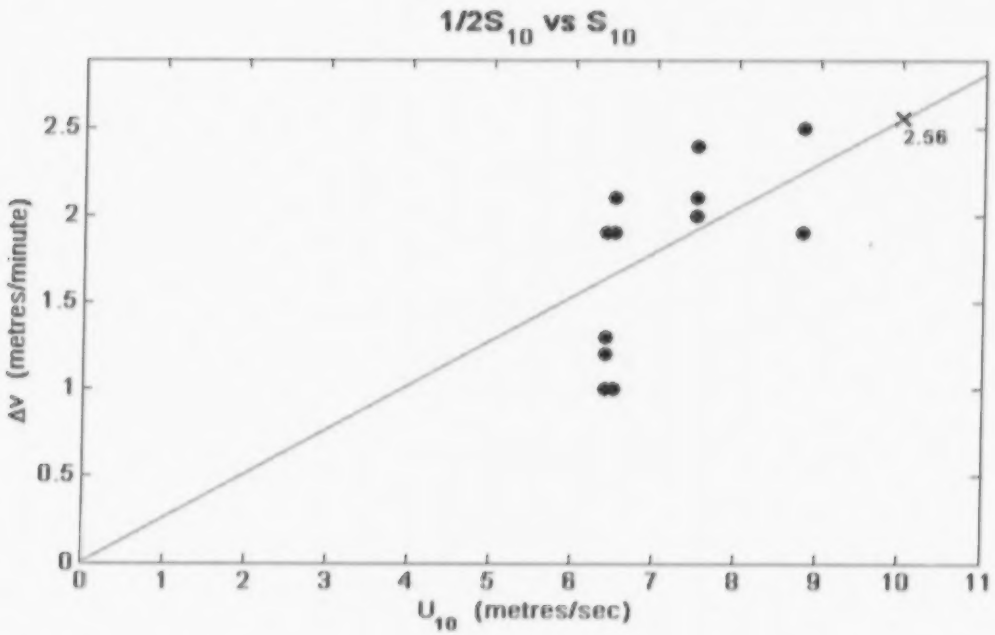


Figure A10: Scatter plot of the separation velocity, $\Delta v$, between the reference $S_{10}$ and the buoy $1/2S_{10}$. The solid line is a least square line. The data are for 4 trials.

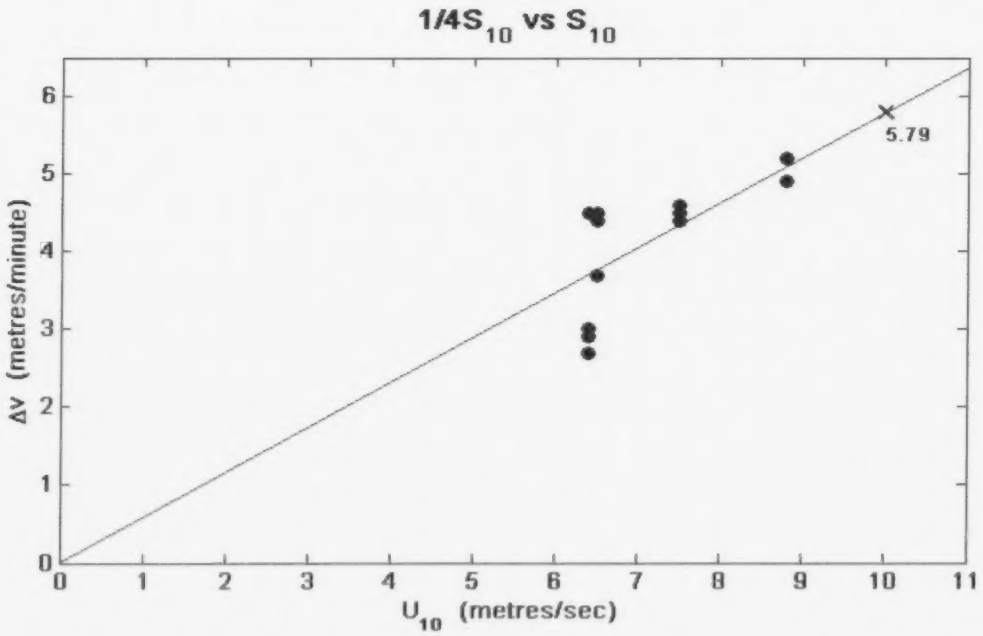


Figure A11: Scatter plot of the separation velocity, $\Delta v$, between the reference $S_{10}$ and the buoy $1/4S_{10}$. The solid line is a least square line. The data are for 4 trials.

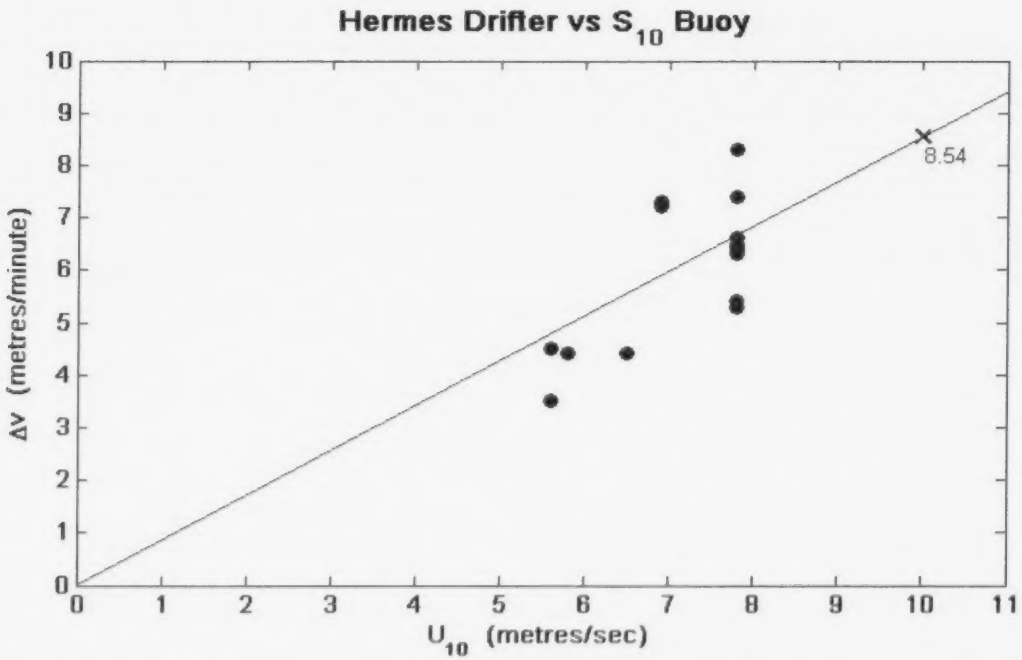


Figure A12: Scatter plot for the Hermes Drifter showing the separation speed, Δv, with reference buoy $S_{10}$ as a function of wind speed. The data are for 6 trials.

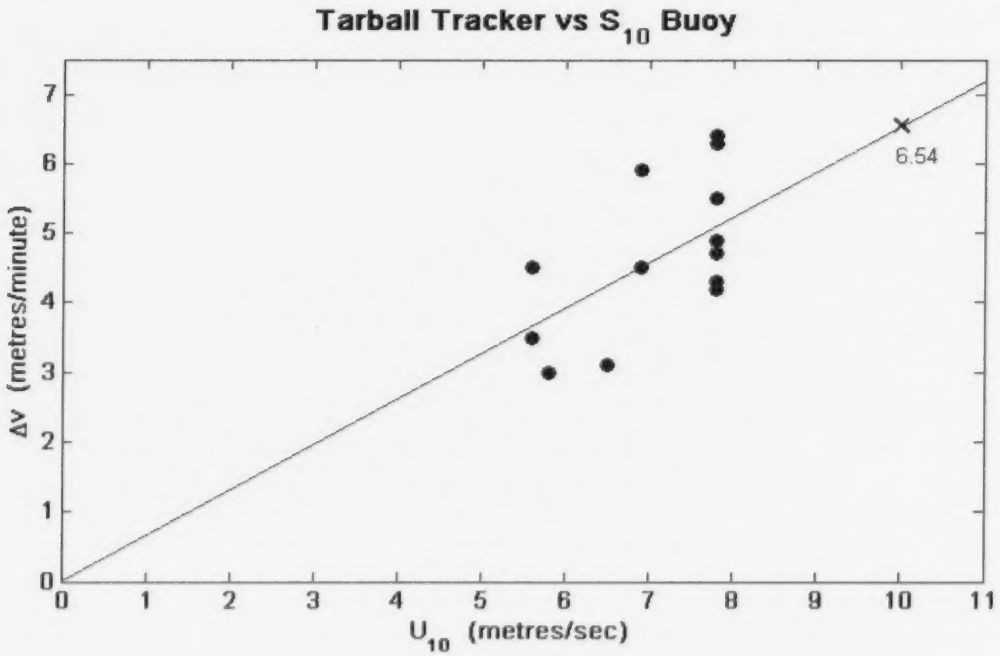


Figure A13: Scatter plot for the Tarball Tracker showing the separation speed, Δv, with reference buoy $S_{10}$ as a function of wind speed. The data are for 6 trials.

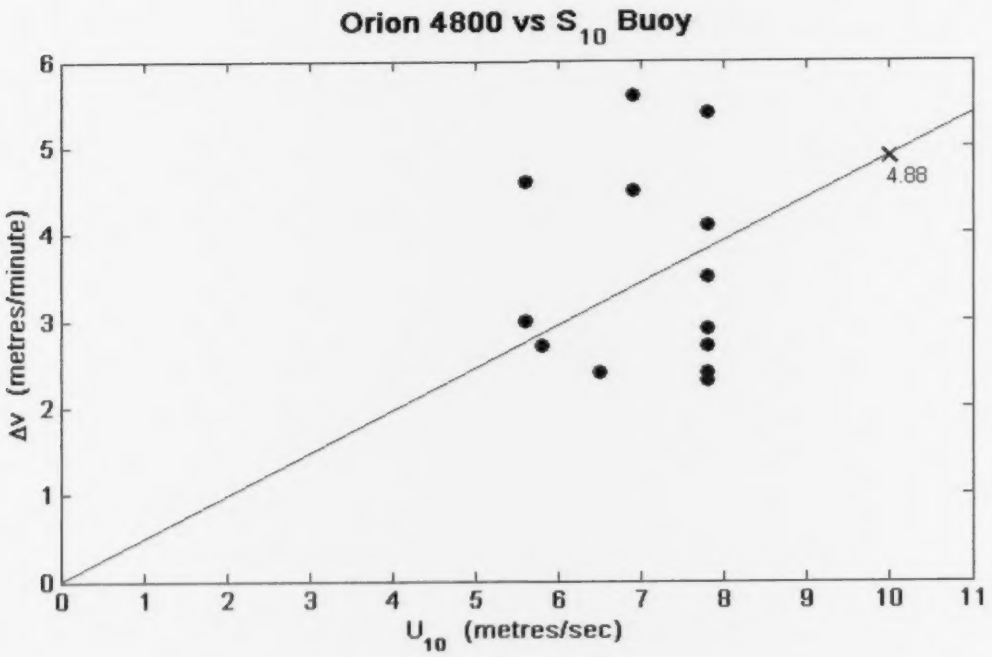


Figure A14: Scatter plot for the Orion 4800 showing the separation speed, Δv, with reference buoy $S_{10}$ as a function of wind speed. The data are for 6 trials.

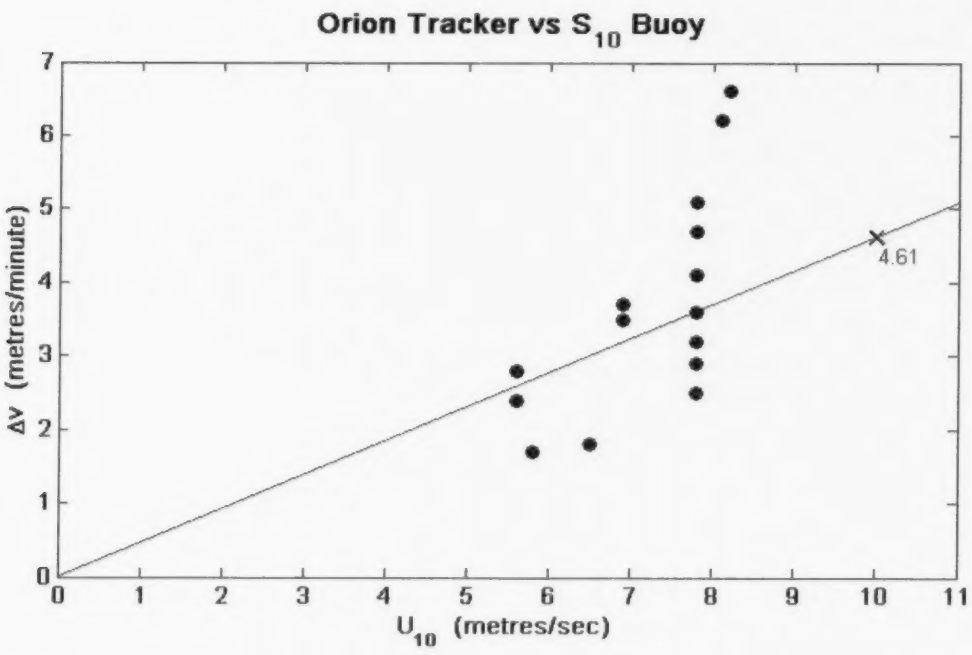


Figure A15: Scatter plot for the Orion Tracker showing the separation speed, Δv, with reference buoy $S_{10}$ as a function of wind speed. The data are for 8 trials.

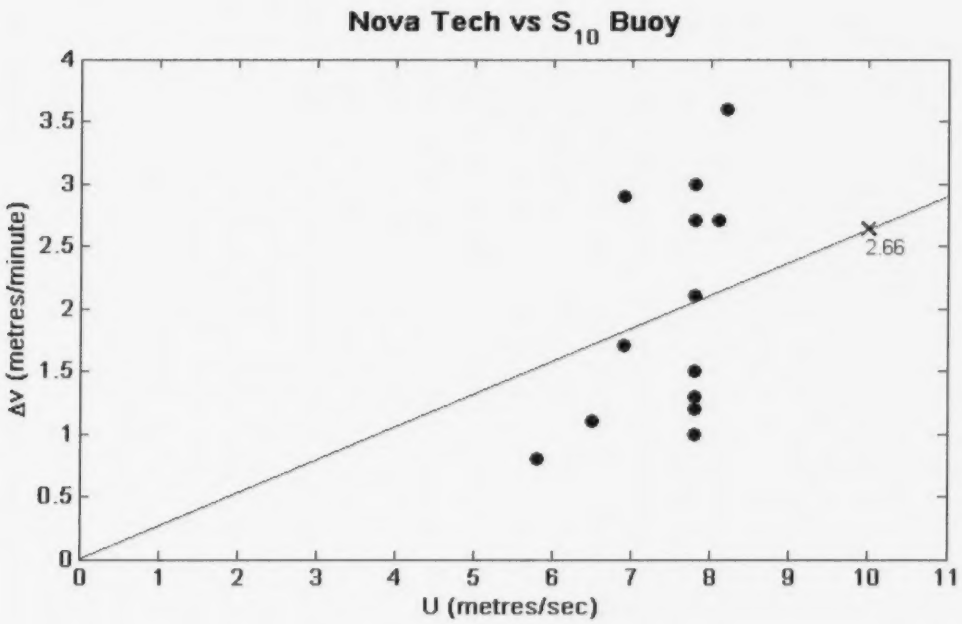


Figure A16: Scatter plot for the Nova Tech showing the separation speed, Δv, with reference buoy $S_{10}$ as a function of wind speed. The data are for 7 trials.